KU LEUVEN

11th World Congress on Computational Mechanics
Barcelona, Spain, 21-25 July 2014

Design and performance of a stiff wave barrier in the soil using 2.5D and 3D FE-BE models

P. Coulier[1], S. François[1], V. Cuéllar[2], G. Degrande[1] and G. Lombaert[1]

[1] Department of Civil Engineering, KU Leuven, Belgium
[2] CEDEX, Madrid, Spain

Introduction

- EU FP7 project RIVAS "Railway Induced Vibration Abatement Solutions" (2011-2013).
- The project aims to reduce environmental vibration by providing a set of mitigation measures at the source, the track, the propagation path and the vehicle.
- 26 partners (railway operators, industry, consultancy, academics), coordination by UIC.
- www.rivas-project.eu
- **WP4 Mitigation measures on transmission/propagation.**
  - Trenches and buried wall barriers.
  - Subgrade stiffening.
  - Wave impeding blocks.
  - Masses along the surface (wave reflectors).

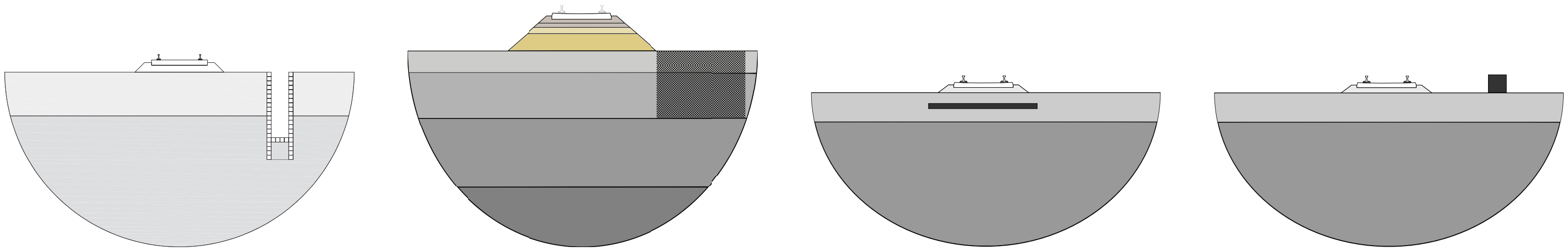

El Realengo test site

Test and reference site

- Conventional railway line (ADIF) between Murcia and Alicante.
- Construction of a new HST line between Madrid and Levante.
- Low Segura river flood plain.
- Construction of a jet grouting wall as a wave impeding barrier.

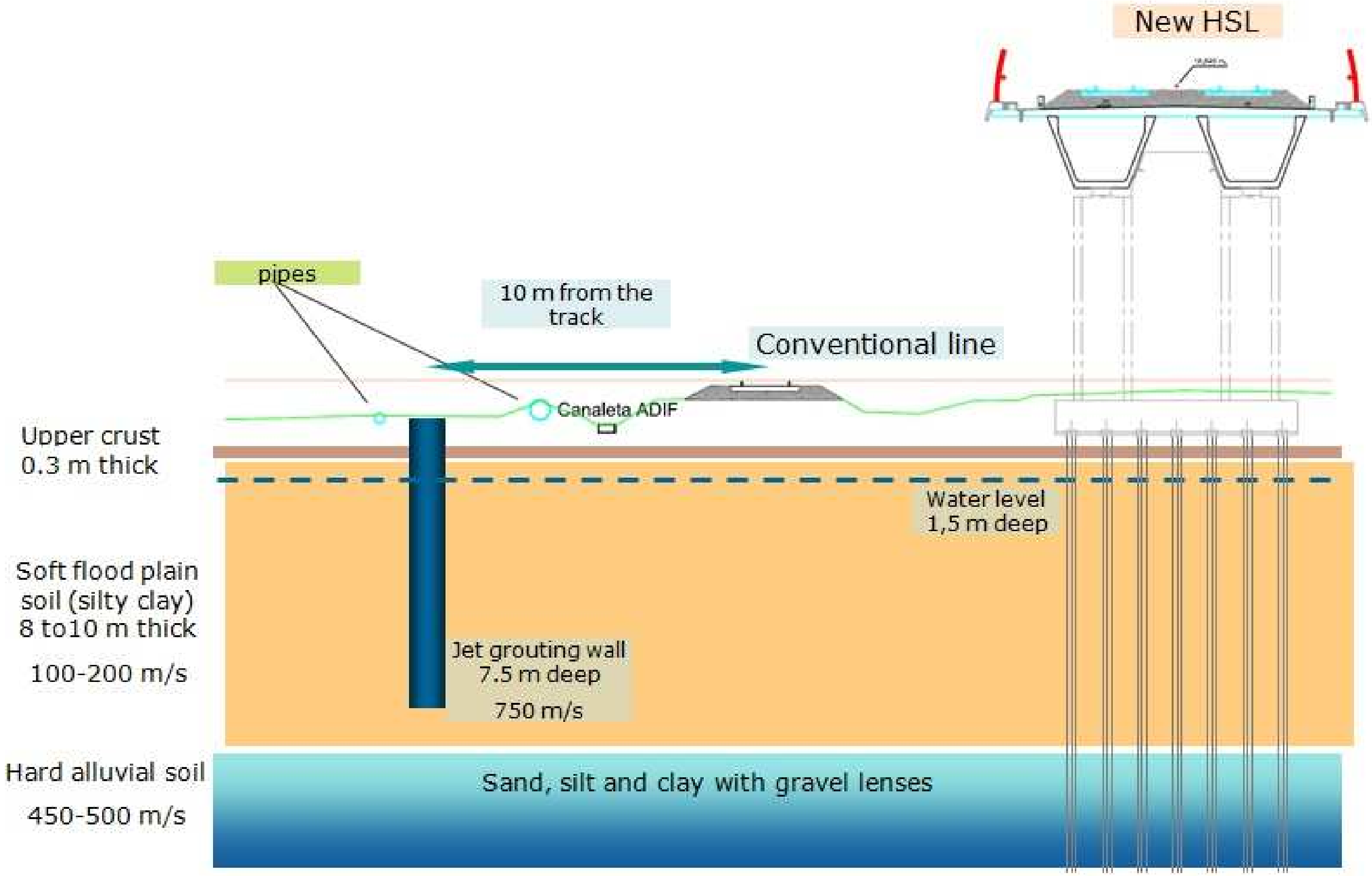

Stiff wave barrier next to the track

- Jet grouting wall next to track as a wave impeding barrier for railway induced vibrations.

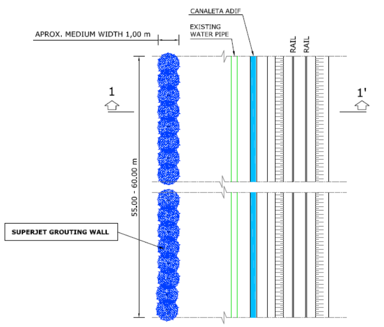

SUPERJET GROUTING WALL LAYOUT

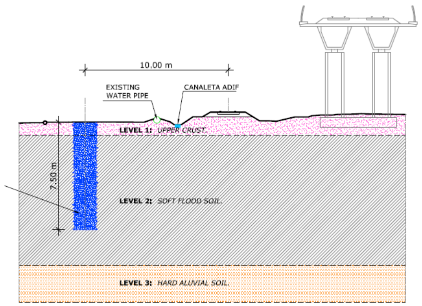

SECCIÓN 1-1'.

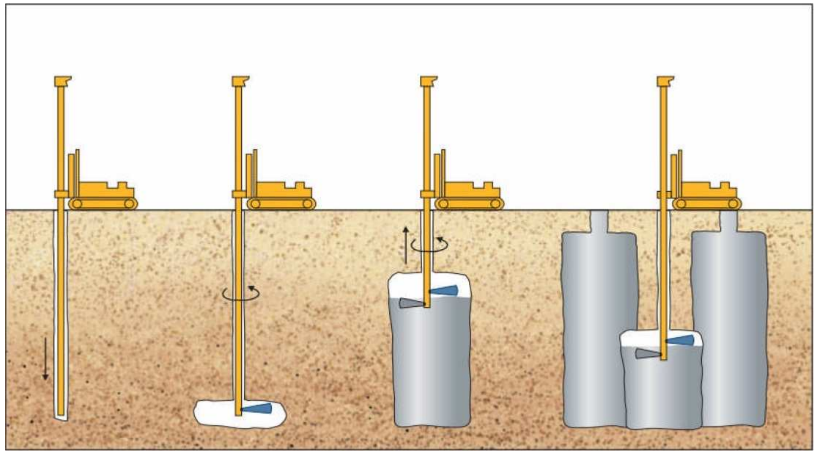

- Common construction techniques:
  - deep vibro compaction;
  - gravel/cement columns;
  - hydraulic fracture injection with stable cement–bentonite mixtures.

Problem outline

- Block of stiffened soil with square cross section (e.g. by means of jet grouting) embedded in a homogeneous halfspace next to a track on embankment [Coulier et al., SDEE, 2013].

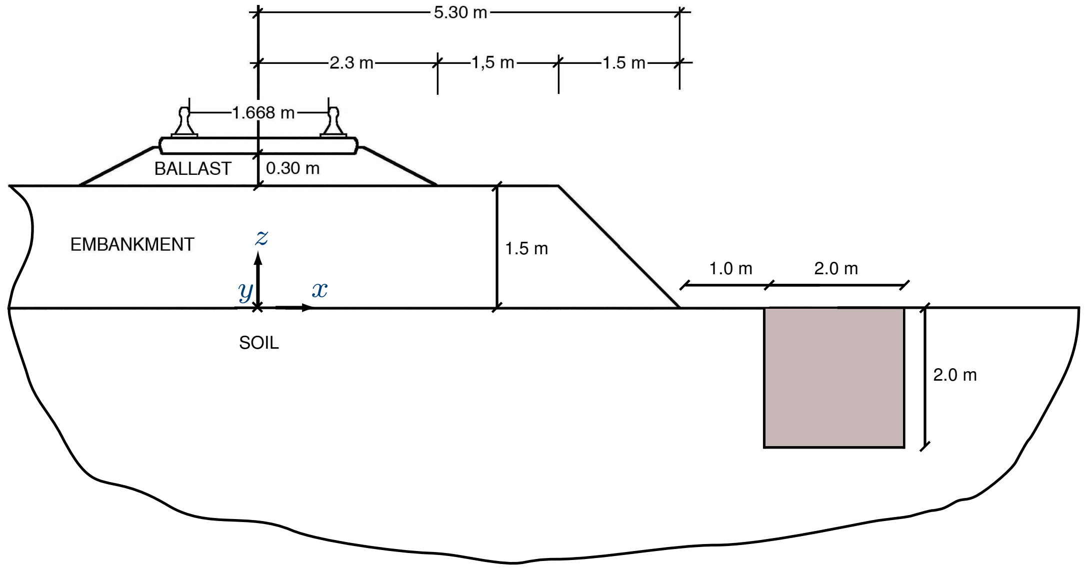

	C_s $[\mathrm{m/s}]$	C_p $[\mathrm{m/s}]$	β_s $[-]$	β_p $[-]$	ρ $[\mathrm{kg/m^3}]$
Halfspace	200	400	0.025	0.025	2000
Stiffened soil	550	950	0.050	0.050	2000

2.5D coupled FE–BE methodology

- Computationally efficient 2.5D approach in the frequency–wavenumber domain:
  - Forward Fourier transform from y to k_y:

$$\tilde{f}(k_y) = \mathscr{F}\left[f(y), k_y\right] = \int_{-\infty}^{+\infty} f(y) \exp\left(ik_y y\right) \, \mathrm{d}y \tag{1}$$

  - 2.5D FE–BE equations [François et al., CMAME, 2010]:

$$\left[\tilde{\mathbf{K}}(k_y,\omega) + i\omega\mathbf{C} - \omega^2\mathbf{M} + \tilde{\mathbf{K}}^{\mathrm{s}}(k_y,\omega)\right] \underline{\tilde{\mathbf{u}}}(k_y,\omega) = \underline{\tilde{\mathbf{f}}}(k_y,\omega) + \underline{\tilde{\mathbf{f}}}^{\mathrm{s}}(k_y,\omega) \tag{2}$$

  - Inverse Fourier transform from k_y to y:

$$f(y) = \mathscr{F}^{-1}\left[f(k_y), y\right] = \frac{1}{2\pi} \int_{-\infty}^{+\infty} f(k_y) \exp\left(-ik_y y\right) \, \mathrm{d}k_y \tag{3}$$

- (Dis)advantages?
  + computationally efficient
  – invariant geometry

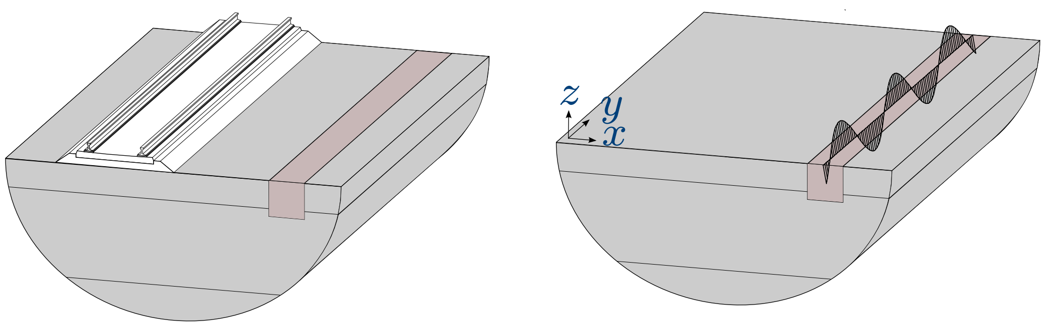

Transfer functions

- Real part of the vertical displacement $\hat{u}_z(\mathbf{x}, \omega)$ without and with barrier and corresponding insertion loss $\widehat{\mathrm{IL}}_z(\mathbf{x}, \omega) = 20 \log_{10} \frac{|\hat{u}_z^{\mathrm{ref}}(\mathbf{x},\omega)|}{|\hat{u}_z(\mathbf{x},\omega)|}$ at (a) $5\,\mathrm{Hz}$, (b) $30\,\mathrm{Hz}$ and (c) $60\,\mathrm{Hz}$.

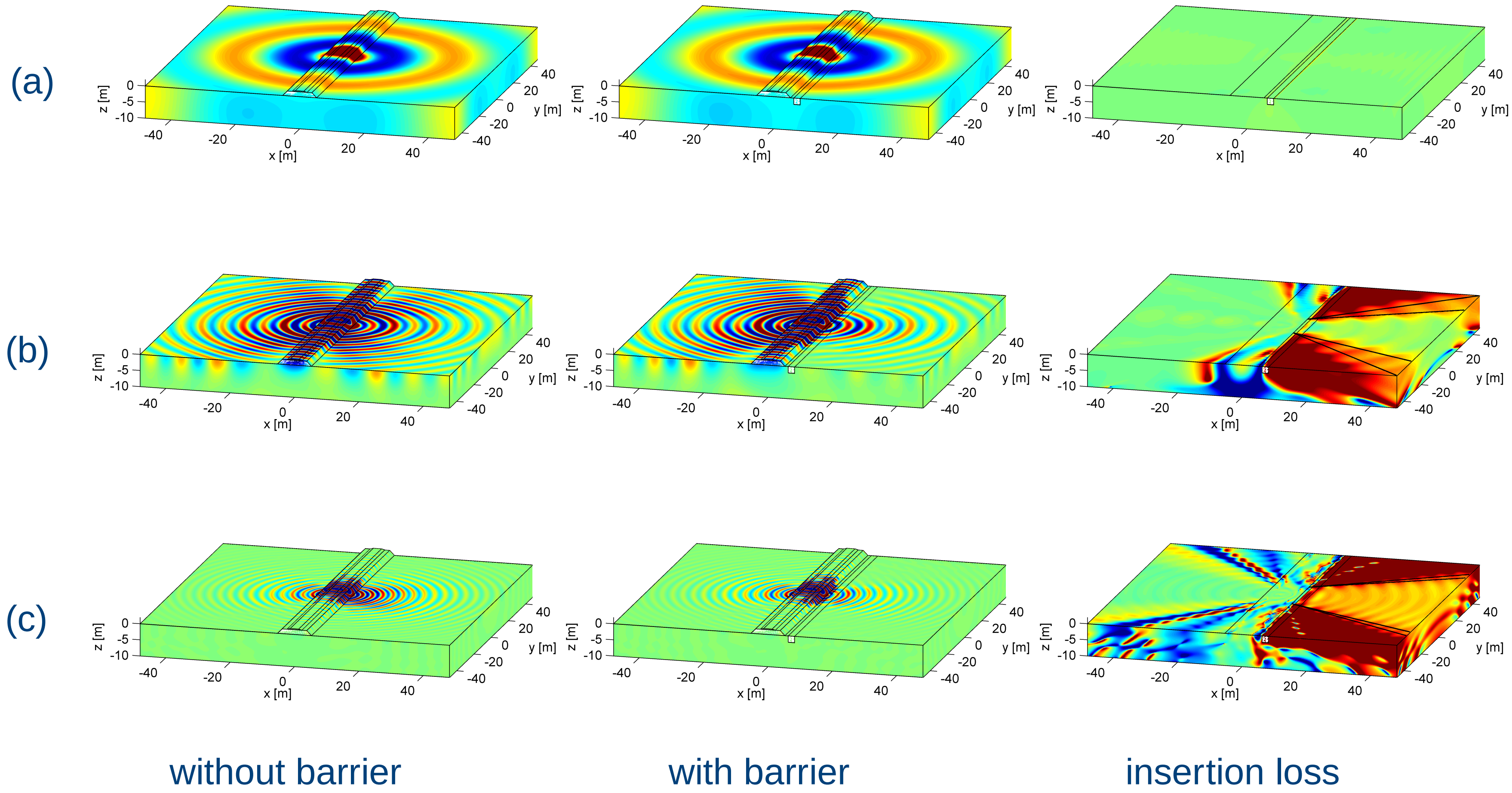

Plane wave propagation

- Plane wave propagation without and with stiff wave barrier for (a) $\lambda_y = \infty$ ($\theta = 0$), (b) $\lambda_\mathrm{R} \leqslant \lambda_y \leqslant \infty$ ($\theta = 0.50$), (c) $\lambda_\mathrm{R} \leqslant \lambda_y \leqslant \infty$ ($\theta = 1.2$), and (d) $\lambda_y < \lambda_\mathrm{R}$ ($\theta = \pi/2$).

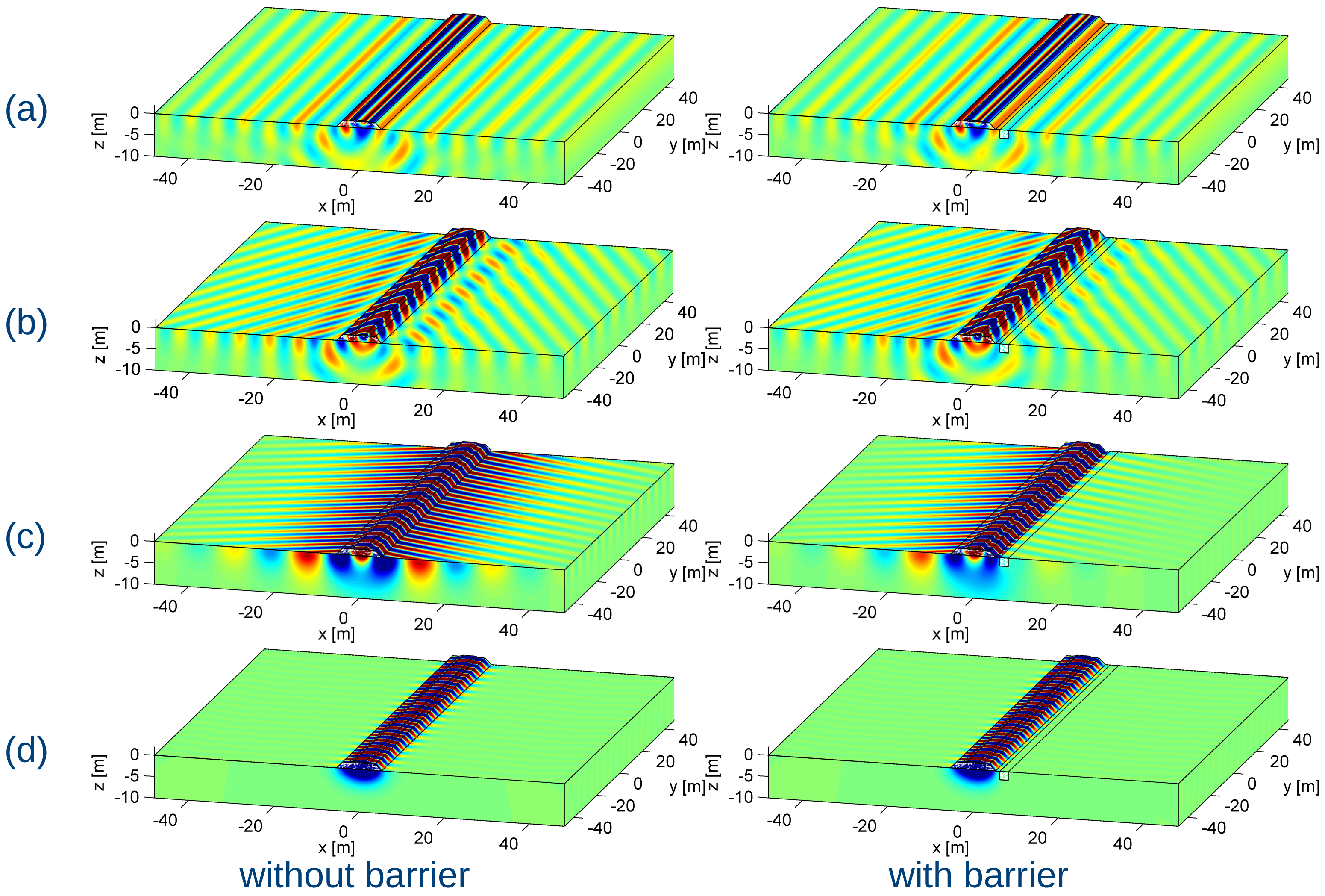

2.5D FE–BE method with spatial windowing

- Spatial windowing technique [Villot et al., JSV, 2001; Coulier et al., SDEE, 2014]:
  - accounts for the structure's finite length
  - maintains the computational efficiency of a 2.5D approach
- Redistribution of the wavenumber spectrum over the entire wavenumber domain:

$$\underline{\tilde{\mathbf{u}}}_{\mathrm{sw}}(k_y,\omega) = \int_{y_1}^{y_2} \underline{\hat{\mathbf{u}}}(y,\omega) \exp(ik_y y)\, \mathrm{d}y = \ldots = \underbrace{\underline{\tilde{\mathbf{u}}}(k_y,\omega)}_{\text{2.5D results}} * \underbrace{\tilde{w}(k_y)}_{\text{windowing}}$$

- Windowing function $\tilde{w}(k_y)$:

$$\tilde{w}(k_y) = \int_{y_1}^{y_2} \frac{1}{2\pi} \exp(ik_y y)\, \mathrm{d}y = \left[\frac{1}{2\pi} \frac{\exp(ik_y y_2)}{ik_y} \left(1 - \exp\left[-ik_y L_y\right]\right)\right]$$

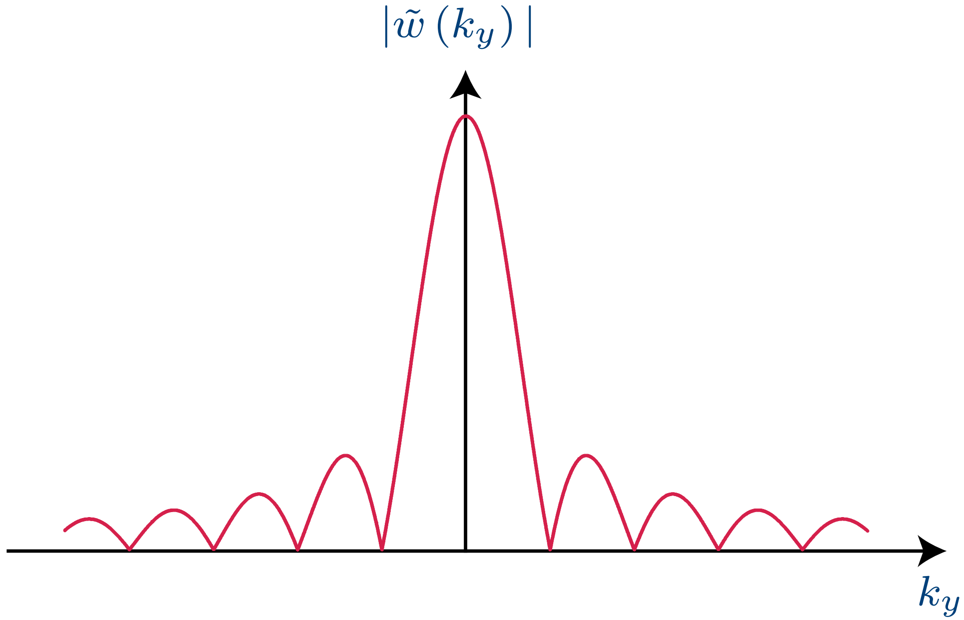

3D FE–$\mathscr{H}$-BE method

- $\mathscr{H}$–matrices: algebraic approximation of the dense BE matrices [Hackbusch, Computing, 1999; Coulier et al., EABE, 2013]

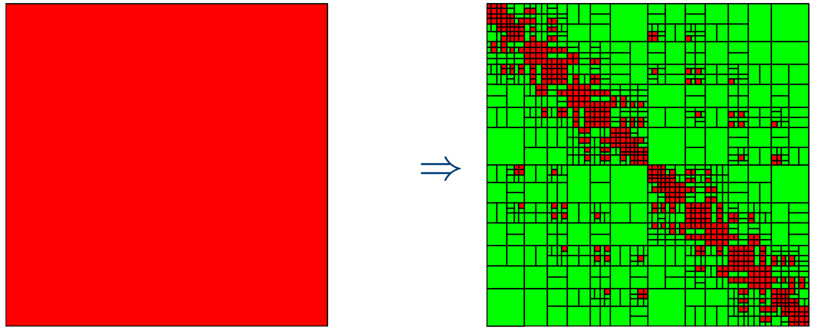

- Iterative FE–$\mathscr{H}$-BE coupling: governing equations are solved separately for each subdomain; boundary conditions on Σ are updated until convergence is achieved.

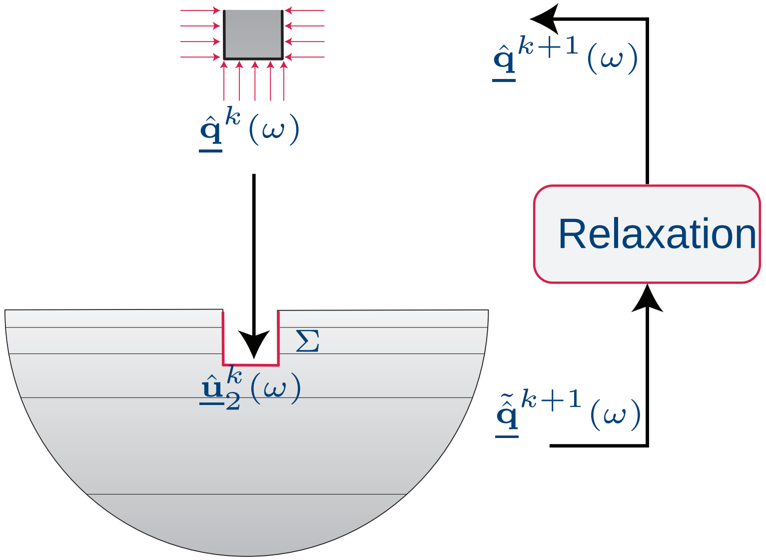

- Sequential Neumann–Dirichlet algorithm [Coulier et al., IJNME, 2014].
- Interface relaxation is crucial: Aitken's Δ^2–method [Aitken, PRSE, 1937].

Stiff wave barrier

2.5D (with spatial windowing) versus 3D calculations

- Vertical displacement $\hat{u}_z(\mathbf{x}, \omega)$ at $30\,\mathrm{Hz}$ for a stiff wave barrier of $2\,\mathrm{m} \times 2\,\mathrm{m}$ embedded in a homogeneous halfspace.

2.5D FE–BE (+ s.w.) | 3D FE–$\mathscr{H}$-BE

$L_y = 15\,\mathrm{m}$

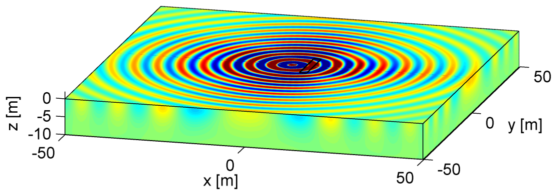

1.10 MB / 0.30 h

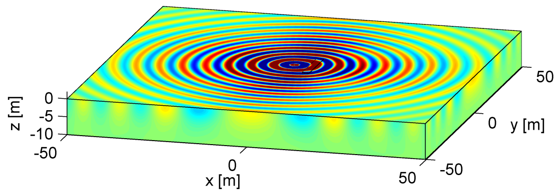

346 MB (736 MB) / 2.3 h

$L_y = 30\,\mathrm{m}$

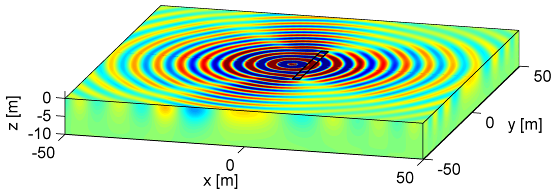

1.10 MB / 0.30 h

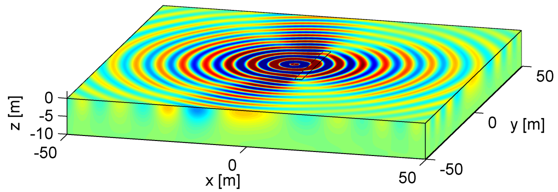

743 MB (2702 MB) / 6.3 h

$L_y = 60\,\mathrm{m}$

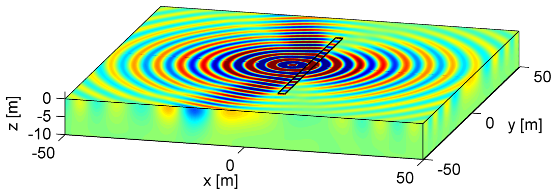

1.10 MB / 0.30 h

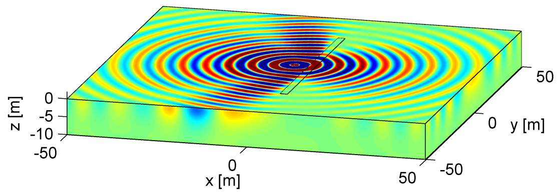

2305 MB (10344 MB) / 12.6 h

$L_y = \infty$

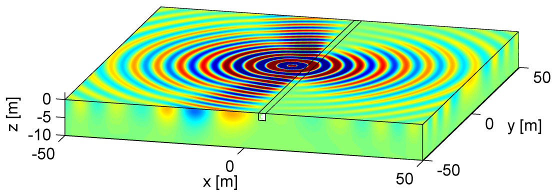

2.5D (with spatial windowing) versus 3D calculations

- Vertical insertion loss $\widehat{\mathrm{IL}}_z(\mathbf{x},\omega)$ at $30\,\mathrm{Hz}$ for a stiff wave barrier of $2\,\mathrm{m} \times 2\,\mathrm{m}$ embedded in a homogeneous halfspace.

2.5D FE–BE (+ s.w.) | 3D FE–$\mathscr{H}$-BE

$L_y = 15\,\mathrm{m}$

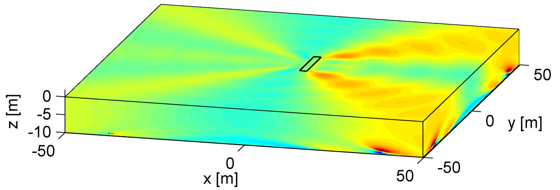

1.10 MB / 0.30 h

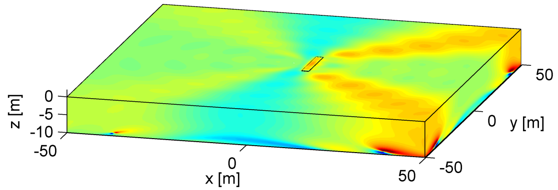

346 MB (736 MB) / 2.3 h

$L_y = 30\,\mathrm{m}$

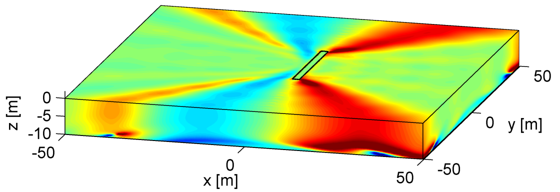

1.10 MB / 0.30 h

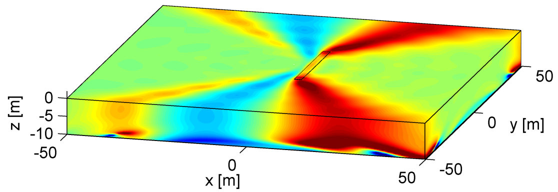

743 MB (2702 MB) / 6.3 h

$L_y = 60\,\mathrm{m}$

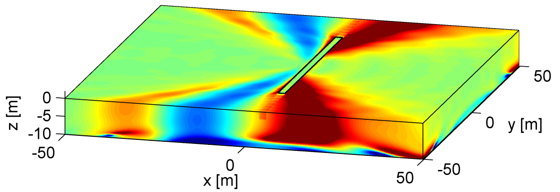

1.10 MB / 0.30 h

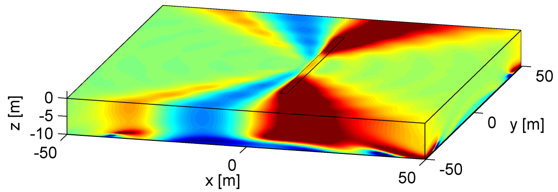

2305 MB (10344 MB) / 12.6 h

$L_y = \infty$

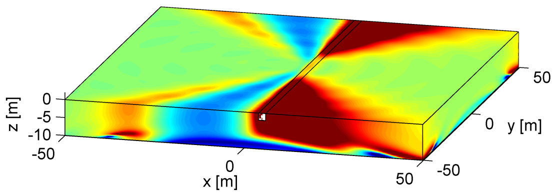

Experimental validation

- A continuous stiff wave barrier of $1\,\mathrm{m} \times 7.5\,\mathrm{m} \times 55\,\mathrm{m}$ has been installed in El Realengo (Spain) within the EU FP7 project RIVAS ("Railway Induced Vibration Abatement Solutions")




Shear wave velocity

- Spectral Analysis of Surface Waves (falling weight deflectometer, CEDEX).
- Seismic Cone Penetration Test (down-hole test, CEDEX).

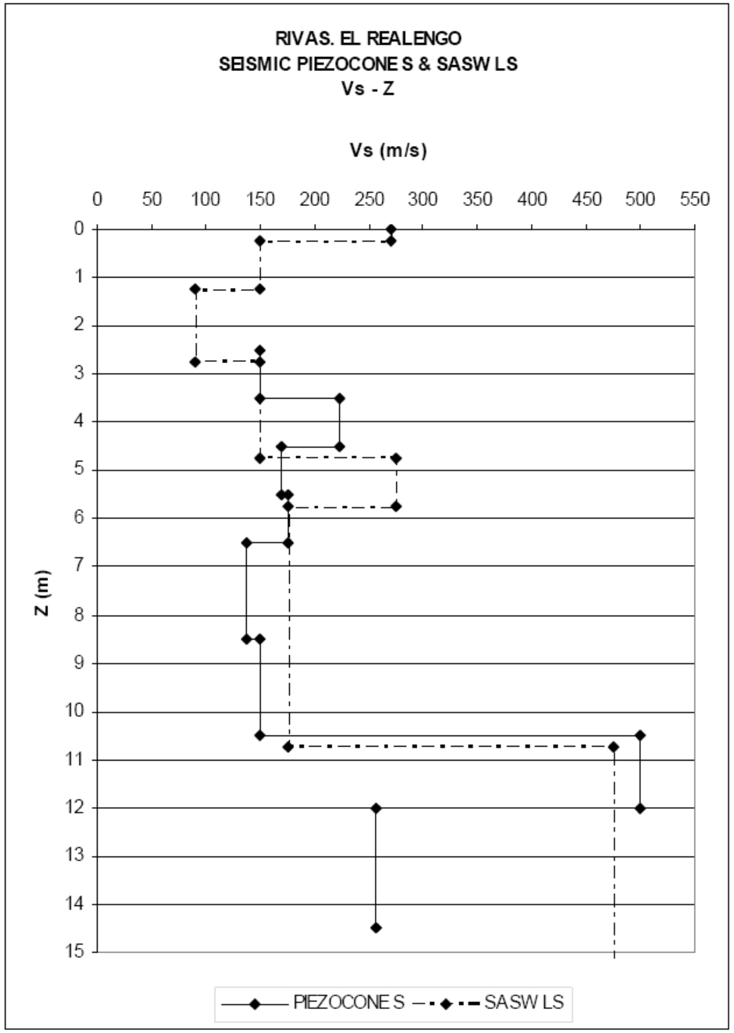

El Realengo test site

Longitudinal wave velocity

- Seismic refraction test (CEDEX).

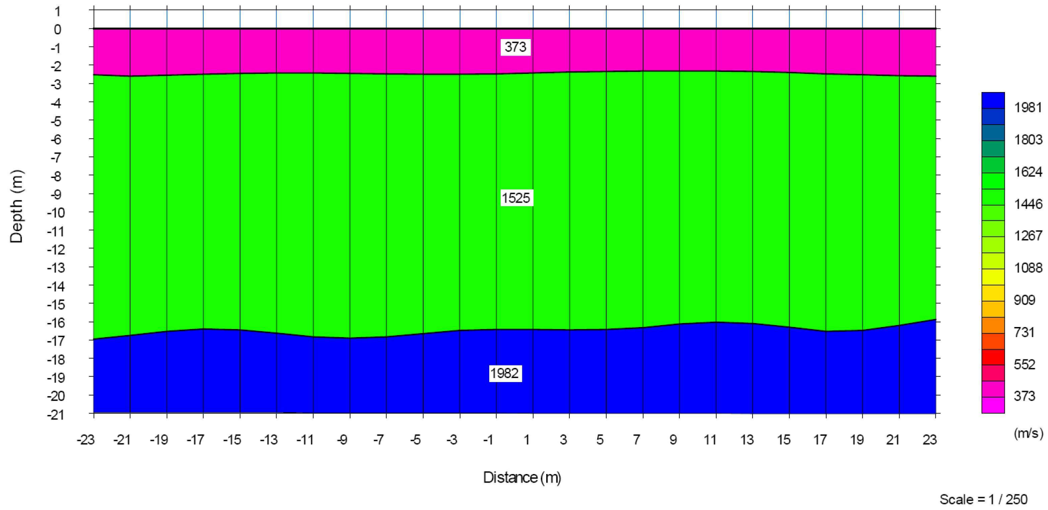

Identified soil profile

Layer	h [m]	C_s [m/s]	C_p [m/s]	β_s [−]	β_p [−]	ρ [kg/m^3]
1	0.30	270	560	0.025	0.025	1800
2	1.20	150	470	0.025	0.025	1750
3	8.50	150	1560	0.025	0.025	1750
4	10.00	475	1560	0.025	0.025	1900
5	∞	550	2030	0.025	0.025	1900

Material damping ratio

- Measured Arias intensity at the test (red line) and reference (green line) section and predicted Arias intensity (a) before and (b) after updating of the material damping ratio [Badsar, 2012].

$$I_{zz}^{\mathrm{E}}(r) = \frac{\pi}{2g}\int_{-\infty}^{+\infty} a^2(r,t)\mathrm{d}t \qquad (4)$$

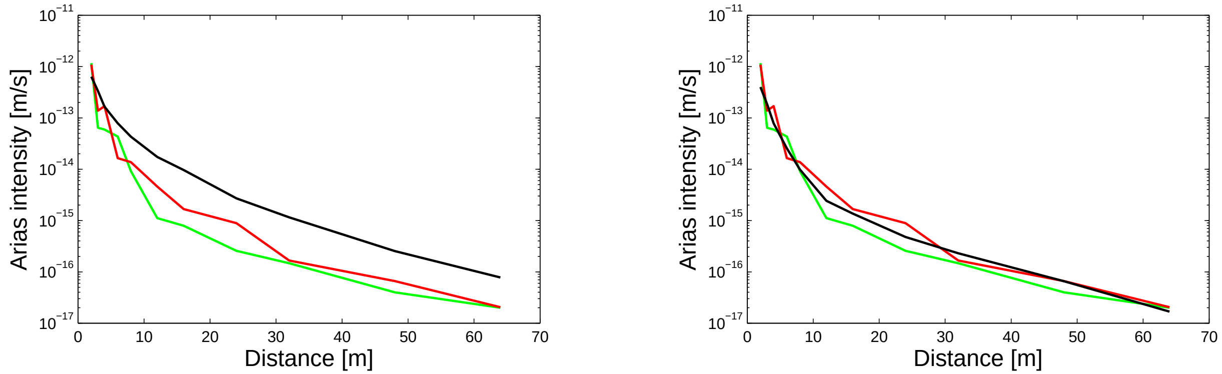

(a) (b)

Identified soil profile (update)

Layer	h $[\mathrm{m}]$	C_{s} $[\mathrm{m/s}]$	C_{p} $[\mathrm{m/s}]$	β_{s} $[-]$	β_{p} $[-]$	ρ $[\mathrm{kg/m^3}]$
1	0.30	270	560	0.123	0.123	1800
2	1.20	150	470	0.112	0.112	1750
3	8.50	150	1560	0.014	0.014	1750
4	10.00	475	1560	0.010	0.010	1900
5	∞	550	2030	0.010	0.010	1900

Track characteristics

- RN 45 rails:
  $EI_{\mathrm{r}} = 3.00 \times 10^6$ Nm^2 and $\rho A_{\mathrm{r}} = 44.8$ kg/m.
- Bi-block reinforced concrete sleepers:
  $m_{\mathrm{sl}} = 200$ kg and spacing $d = 0.6$ m.
- Rubber rail pads with a thickness of 4.5 mm and stiffness of 300 kN/mm.
- Ballast layer:
  $d = 0.50$ m, $C_{\mathrm{s}} = 250$ m/s, $\nu = 0.2$ and $\rho = 1600$ kg/m^3.
- Embankment:
  $d = 0.50$ m, $C_{\mathrm{s}} = 200$ m/s, $\nu = 0.35$ and $\rho = 1700$ kg/m^3.

Jet grouting wall dimensions

- Variant A: $w = 1\,\mathrm{m}$, $h = 5\,\mathrm{m}$

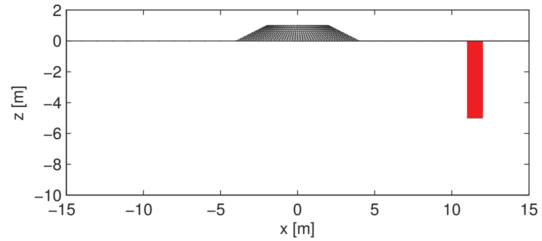

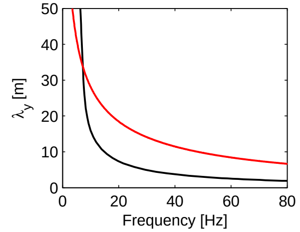

- Variant B: $w = 1\,\mathrm{m}$, $h = 7.5\,\mathrm{m}$

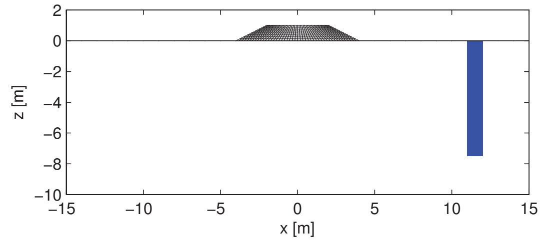

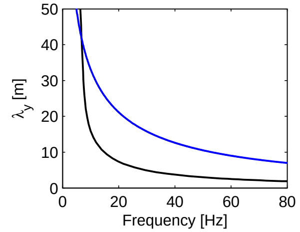

- Variant C: $w = 1\,\mathrm{m}$, $h = 10\,\mathrm{m}$

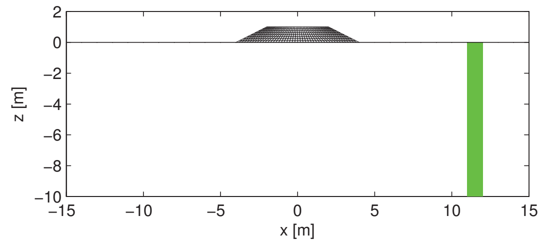

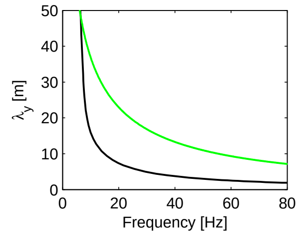

C_s [m/s]	C_p [m/s]	β_s [−]	β_p [−]	ρ [kg/m^3]
650	1125	0.030	0.030	2200

El Realengo test site

2.5D coupled FE-BE calculations

- Real part of the vertical displacement $\hat{u}_z(\mathbf{x}, \omega)$ at (a) $5\,\mathrm{Hz}$, (b) $30\,\mathrm{Hz}$ and (c) $60\,\mathrm{Hz}$ without and with barrier and insertion loss for variant A.

(a)
(b)
(c)

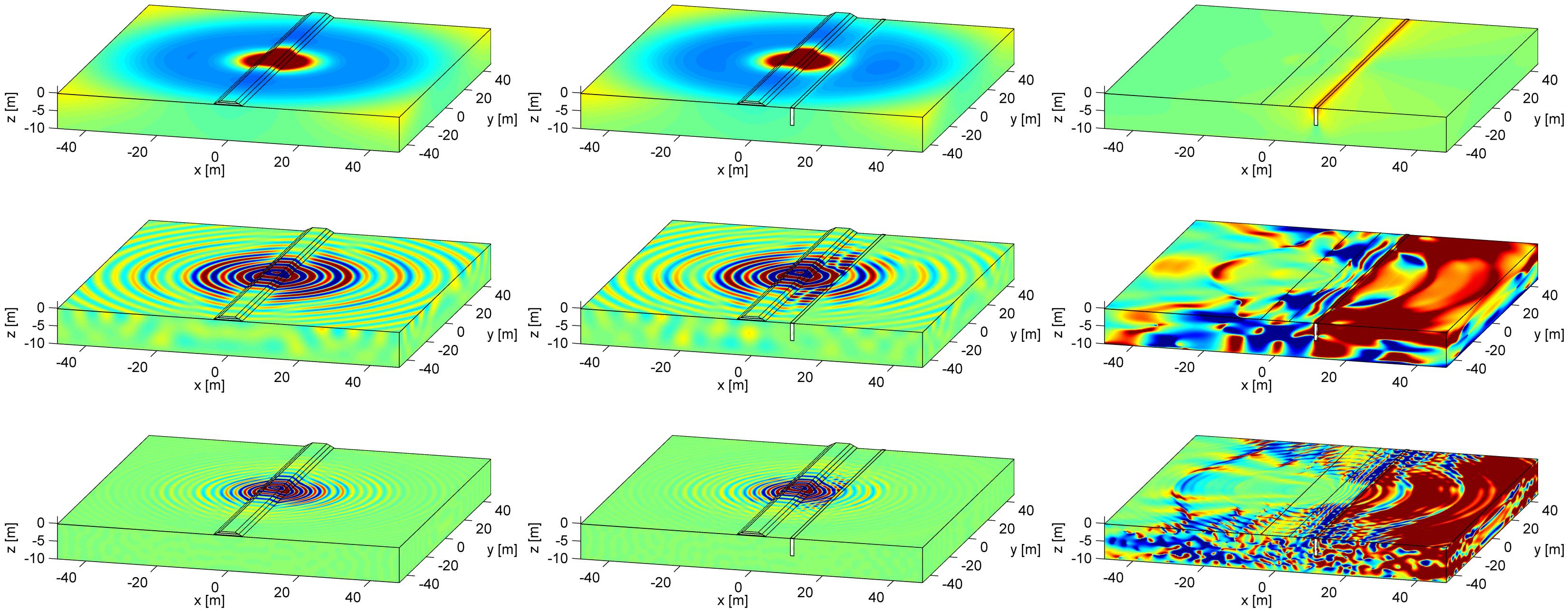

without barrier | with barrier | insertion loss

El Realengo test site

Experimental validation

- Passage of a Renfe S599 long distance train.

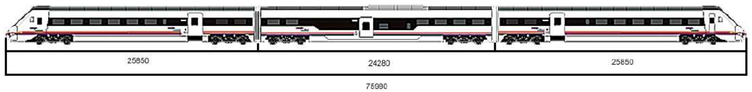

- Simplified vehicle model, only the unsprung masses are taken into account: $M_\mathrm{u} = 1940\,\mathrm{kg}$ for motor coaches and $M_\mathrm{u} = 1704\,\mathrm{kg}$ for central carriage.
- Hertzian contact spring: $k_\mathrm{Hz} = 3 \times 10^9\,\mathrm{N/m}$.
- Track unevenness: FRA class 1 (poor track quality).
- Train speed: $v = 118\,\mathrm{km/h}$.

Experimental validation

- Measurement points at test and reference site.

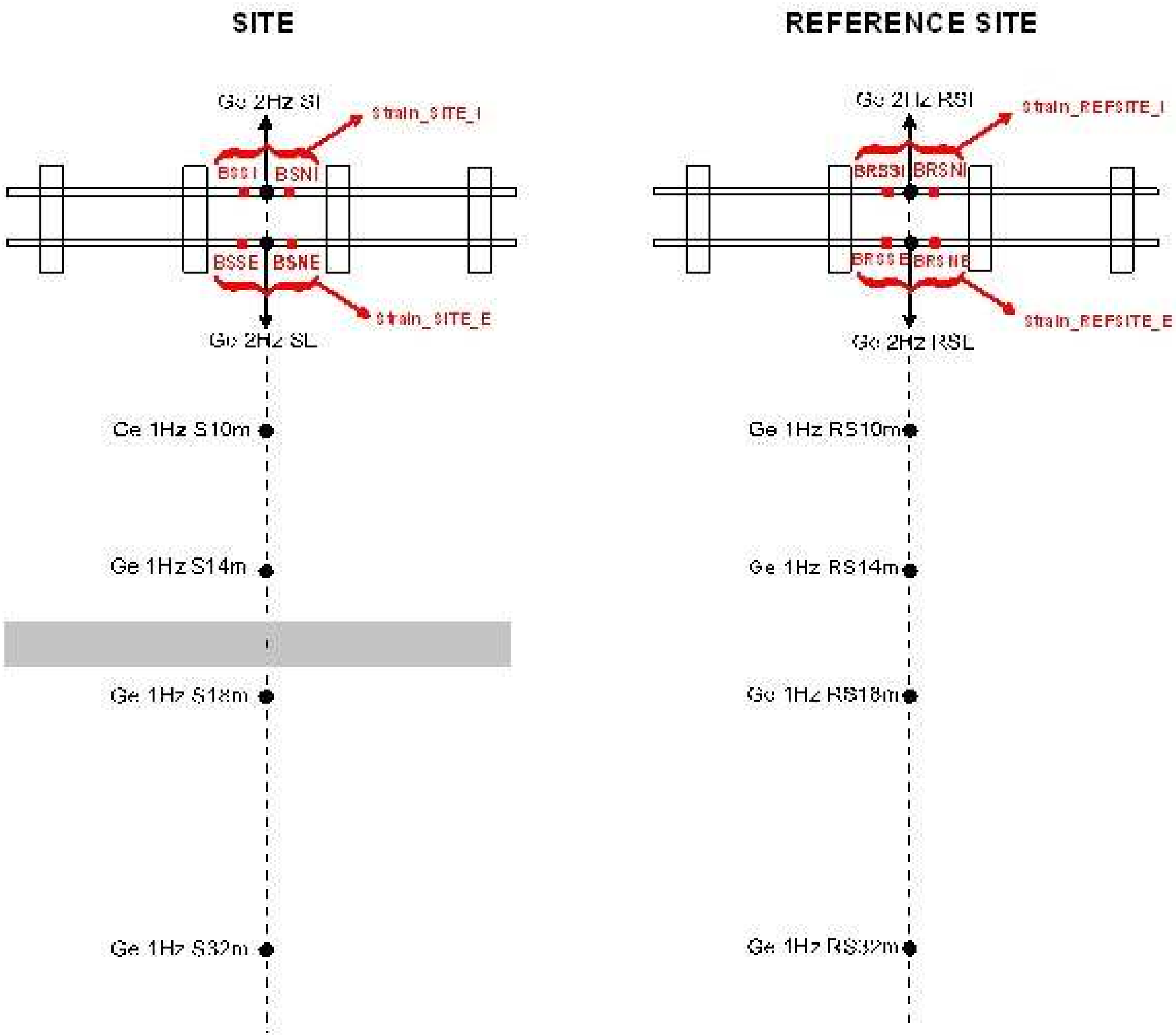

Experimental validation

- Test site and reference site.

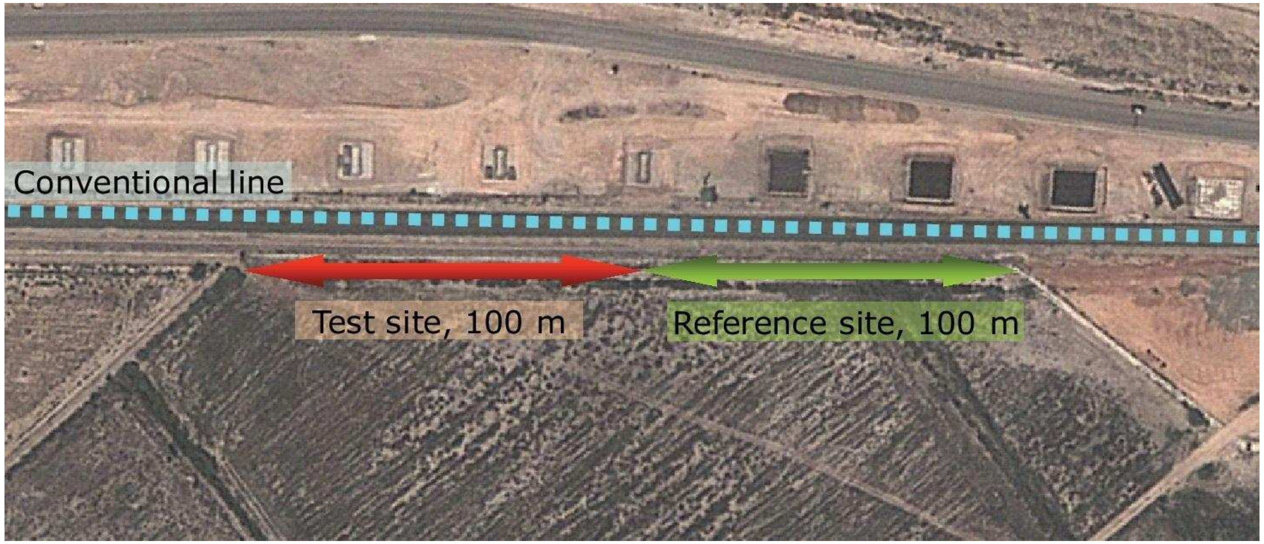

- Measured free field velocity at (a) $18\,\mathrm{m}$ and (b) $32\,\mathrm{m}$ from the track center at the *reference site* and at the *test site* during the passage of a Renfe S599 train at a speed of $117\,\mathrm{km/h}$. The barrier is situated at $16.2\,\mathrm{m}$ from the track center.

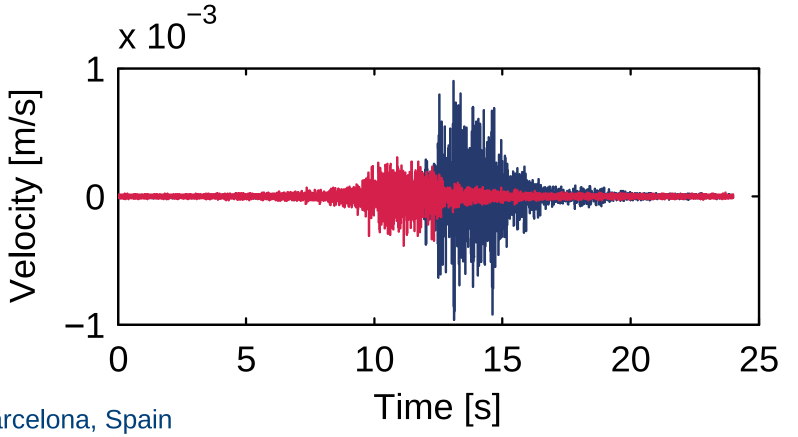

(a)

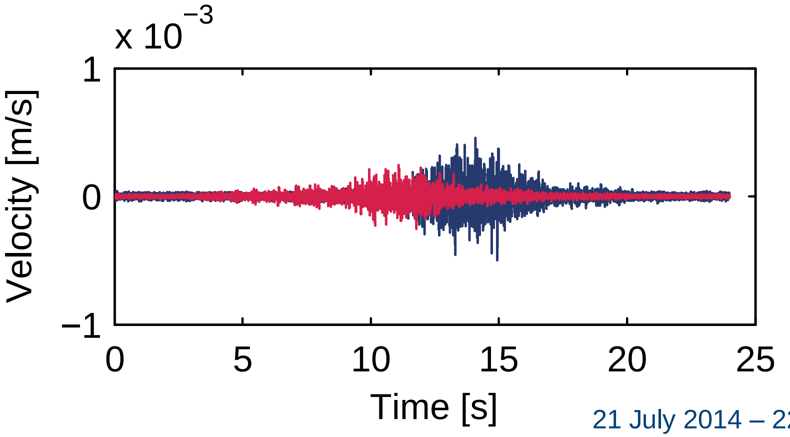

(b)

El Realengo test site

Experimental validation

- Measured vibration velocity level due the passage of Renfe S599 trains at an average speed of $118\,\mathrm{km/h}$ at the *reference site* and at the *test site* before (dashed line) and after (solid line) installation of the barrier, at (a) $10\,\mathrm{m}$, (b) $14\,\mathrm{m}$, (c) $18\,\mathrm{m}$, and (d) $32\,\mathrm{m}$ from the track center. The barrier is situated at $16.2\,\mathrm{m}$ from the track center.

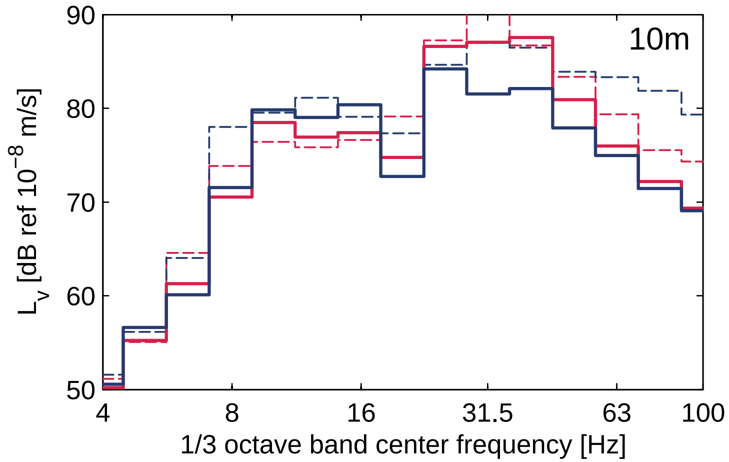

(a)

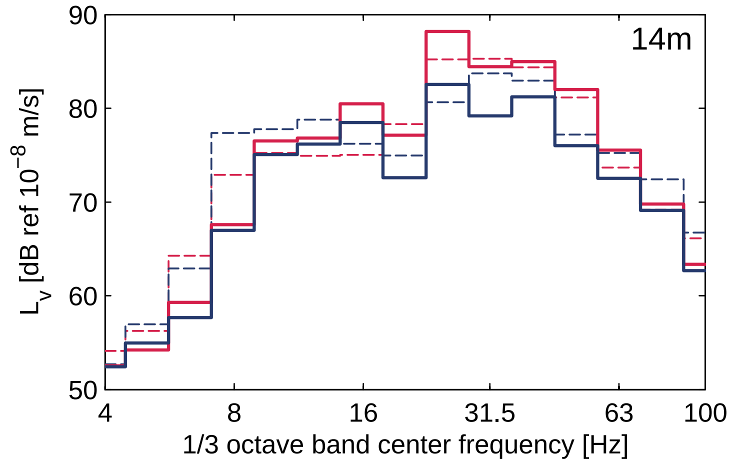

(b)

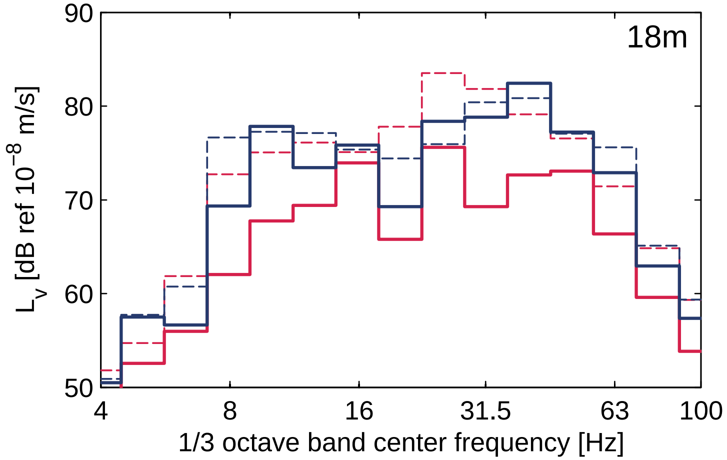

(c)

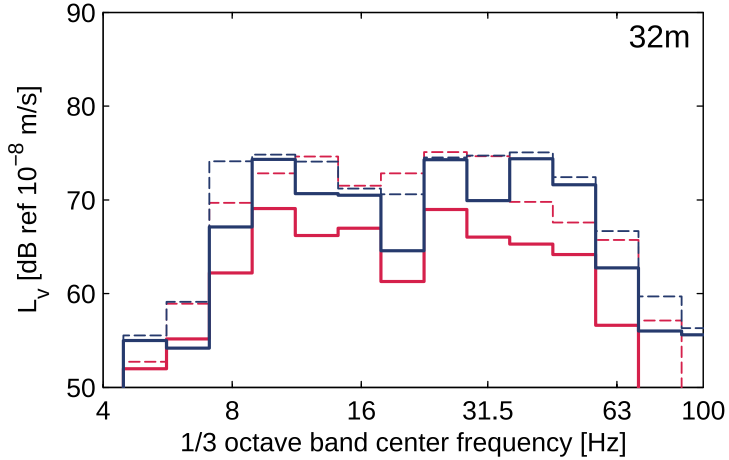

(d)

Experimental validation

- *Predicted* and *measured* vertical insertion loss for RENFE S599 trains at an average speed of $118\,\mathrm{km/h}$ at (a) $10\,\mathrm{m}$, (b) $14\,\mathrm{m}$, (c) $18\,\mathrm{m}$, and (d) $32\,\mathrm{m}$ from the track center. The barrier is situated at $16.2\,\mathrm{m}$ from the track center.

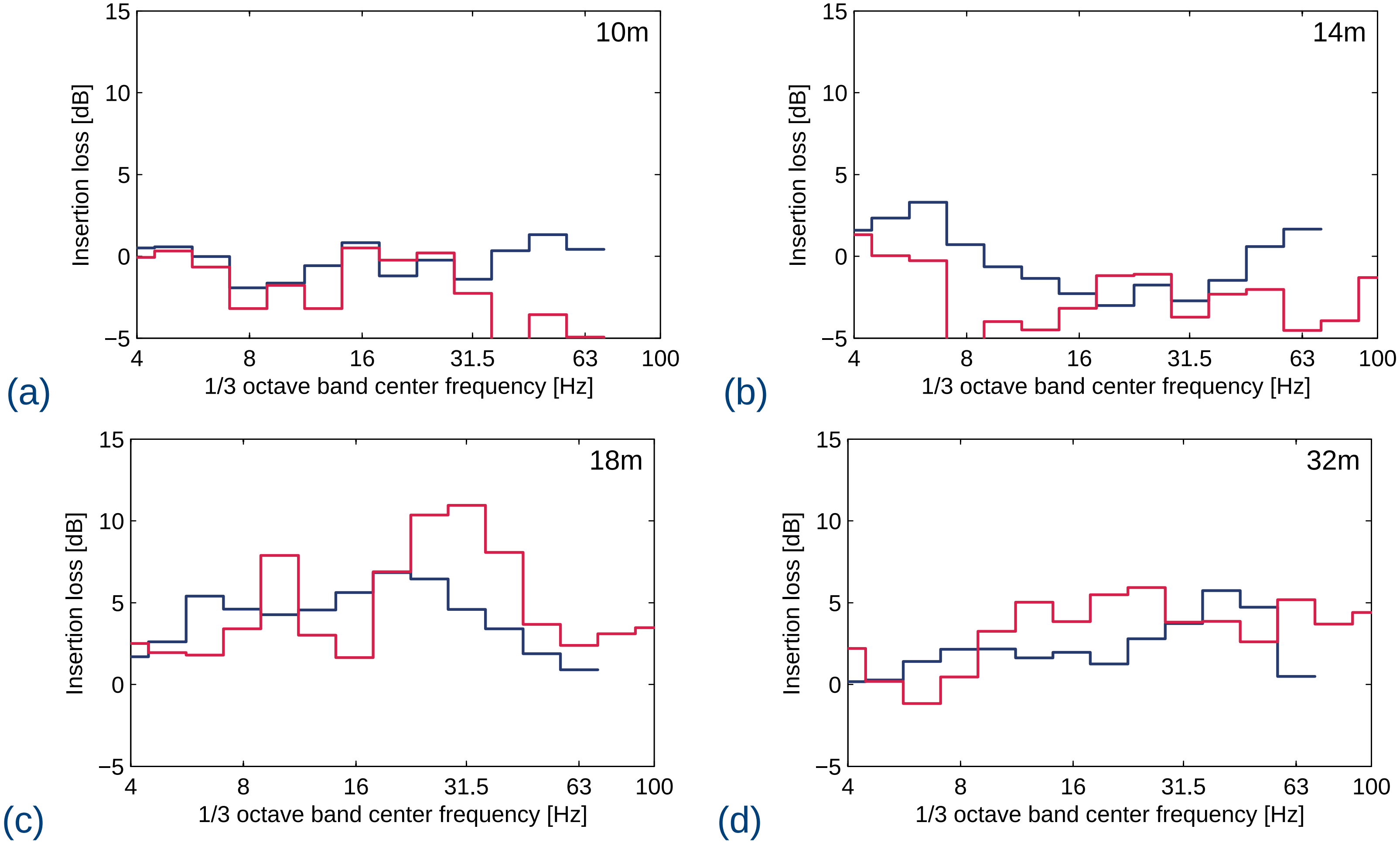

Conclusion

- Stiff wave barrier can behave as a wave impeding barrier at sites with soft soil layers.
- The wave impeding effect critically depends on the relation between λ_{R} and λ_{b}:
  - A reduction of vibration levels is only possible above a critical frequency f_{c} (if $\lambda_{\mathrm{b}} > \lambda_{\mathrm{R}}$).
  - Area of significant reduction is delimited by $\theta_{\mathrm{c}}(\omega) = \sin^{-1}\left(\lambda_{\mathrm{R}}/\lambda_{\mathrm{b}}\right)$

  $\Rightarrow$ expressions for f_{c} and $\theta_{\mathrm{c}}(\omega)$ are very useful in an early design stage.
- Stiff wave barrier should be as stiff, deep, heavy and long as possible.
- Numerical prediction using 2.5D (with or without spatial windowing) or 3D coupled FE-BE models are very useful to assess the performance of wave impeding barriers.
- A jet grouting wall has been constructed at a test site near a railway track in El Realengo.
- Insertion loss $\widehat{\mathrm{IL}}_z(\mathbf{x}, \omega)$ is larger closer to the track and at higher frequencies.